

## Triggering of the 1999 $M_W$ 7.1 Hector Mine earthquake by aftershocks of the 1992 $M_W$ 7.3 Landers earthquake

Karen R. Felzer, Thorsten W. Becker, Rachel E. Abercrombie, Göran Ekström, and James R. Rice<sup>1</sup>

Department of Earth and Planetary Sciences, Harvard University, Cambridge, Massachusetts, USA

Received 9 August 2001; revised 19 February 2002; accepted 19 March 2002; published 19 September 2002.

[1] There is strong observational evidence that the 1999  $M_W$  7.1 Hector Mine earthquake in the Mojave Desert, California, was triggered by the nearby 1992  $M_W$  7.3 Landers earthquake. Many authors have proposed that the Landers earthquake directly stressed the Hector Mine fault. Our model of the Landers aftershock sequence, however, suggests there is an 85% chance that the Hector Mine hypocenter was actually triggered by a chain of smaller earthquakes that was initiated by the Landers main shock. We perform our model simulations using the Monte Carlo method based on the Gutenberg-Richter relationship, Omori's law, Båth's law, and assumptions that all earthquakes, including aftershocks, are capable of producing aftershocks and that aftershocks produce their own aftershocks at the same rate that other earthquakes do. In general, our simulations show that if it has been more than several days since an  $M \geq 7$  main shock, most new aftershocks will be the result of secondary triggering. These secondary aftershocks are not physically constrained to occur where the original main shock increased stress. This may explain the significant fraction of aftershocks that have been found to occur in main shock stress shadows in static Coulomb stress triggering studies. *INDEX TERMS:* 7230 Seismology:

Seismicity and seismotectonics; 7223 Seismology: Seismic hazard assessment and prediction; 7209

Seismology: Earthquake dynamics and mechanics; *KEYWORDS:* aftershocks, foreshocks, Hector Mine, Landers, Coulomb

**Citation:** Felzer, K. R., T. W. Becker, R. E. Abercrombie, G. Ekström, and J. R. Rice, Triggering of the 1999  $M_W$  7.1 Hector Mine earthquake by aftershocks of the 1992  $M_W$  7.3 Landers earthquake, *J. Geophys. Res.*, 107(B9), 2190, doi:10.1029/2001JB000911, 2002.

### 1. Introduction

[2] On 16 October 1999, the  $M_W$  7.1 Hector Mine earthquake occurred in the Mojave Desert, California, only 7 years after and 20 km away from the 1992  $M_W$  7.3 Landers earthquake (Figure 1). It is likely that the Landers earthquake triggered the Hector Mine earthquake, since the recurrence interval for  $M > 7$  events in the Mojave Desert is predicted to be several thousand years or more from geodetic measurements [Sauber *et al.*, 1994]. Yet attempts to establish that the Landers earthquake increased the static Coulomb stress at the Hector Mine hypocenter have proven to be inconclusive [Harris, 2000; Harris and Simpson, 2002] and sensitive to the coefficient of friction [Parsons and Dreger, 2000]. This has generated a number of other proposals for the triggering mechanism, including dynamic stressing [Kilb, 2000, 2001], viscoelastic stress transfer [Zeng, 2001; Freed and Lin, 2001; Pollitz and Sacks, 2002], and static stress changes combined with rate and state friction [Price and Bürgmann, 2002].

[3] A critical component of the above works, and of many other earthquake-triggering studies, is that it is assumed that the slip of the main shock alone, or the combined slip of the main shock and a large aftershock, was responsible for all subsequent triggering. In this study, we address the probability that small aftershocks were actually key players in delivering critical stress to the Hector Mine hypocenter. Our analysis is performed using Monte Carlo modeling and is based on the Gutenberg-Richter relationship, Omori's law, Båth's law, and assumptions that all earthquakes are capable of producing aftershocks and that aftershocks produce their own aftershocks at the same rate that other earthquakes of comparable magnitude do. These assumptions are essentially the same as those used in other studies that have modeled secondary aftershock activity, such as Kagan and Knopoff [1981] and Kagan [1991]. With the exception of Båth's law, they are also the same assumptions made by Ogata [1998], Console and Murru [2001], A. Helmstetter and D. Sornette (Subcritical and supercritical regimes in epidemic models of earthquake aftershocks, submitted to *Journal of Geophysical Research*, 2001), and others.

[4] First, we provide evidence that not only are all earthquakes capable of producing aftershocks but that small earthquakes can trigger aftershocks larger than themselves. We then discuss circumstantial evidence that the Hector Mine earthquake was the result of such triggering. Finally,

<sup>1</sup>Also at Division of Engineering and Applied Sciences, Harvard University, Cambridge, Massachusetts, USA.

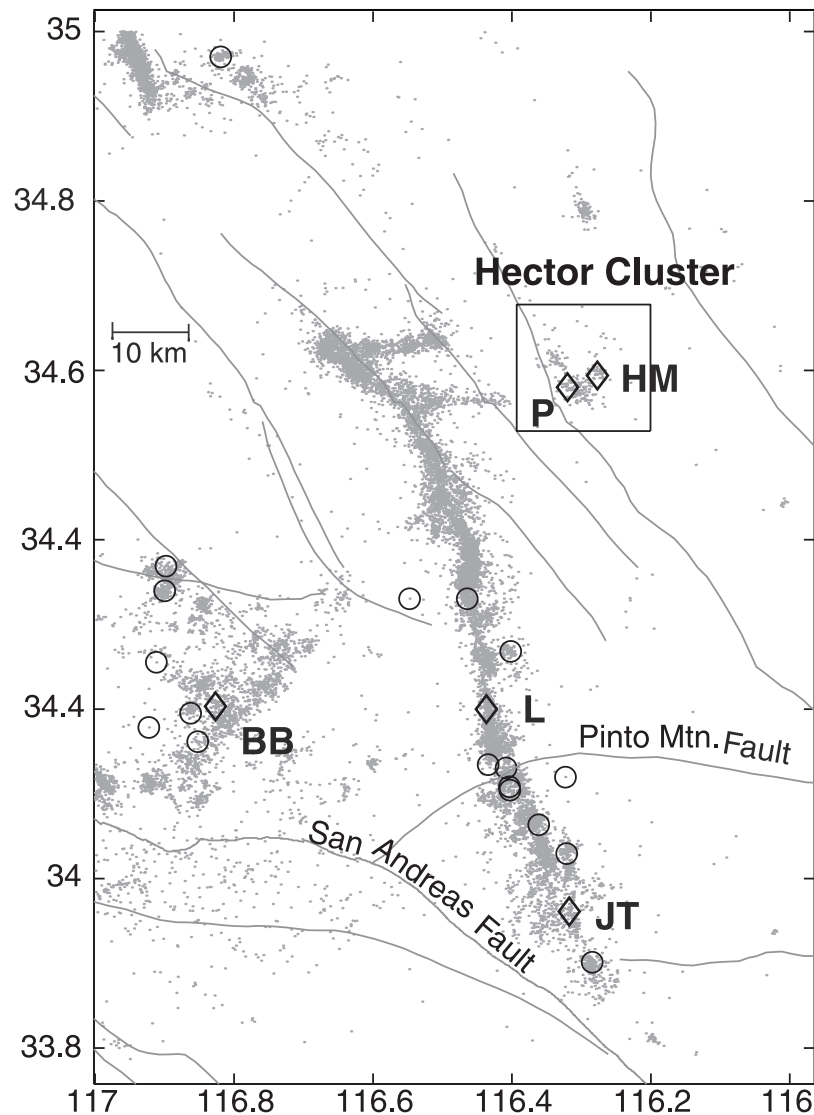


**Figure 1.** Map of recorded Landers aftershocks, occurring from the time of the Landers main shock (28 June 1992) until the Hector Mine main shock (16 October 1999). Gray dots denote the epicenters of all  $M \geq 2$  aftershocks; black circles surround the epicenters of  $M \geq 5$  aftershocks not specifically discussed in the text. Black diamonds denote the epicenters of the Landers (L), Joshua Tree (JT), Big Bear (BB), Pisgah (P), and Hector Mine (HM) earthquakes, as labeled. The box identifies the distinct cluster of Landers aftershocks around the future Hector Mine epicenter.

we use Monte Carlo simulations to calculate a specific probability that the Hector Mine earthquake was a secondary, not direct, aftershock of the Landers earthquake.

## 2. Evidence That Small Earthquakes Can Trigger Larger Ones

[5] The best evidence we have that small earthquakes can trigger large ones is that occasionally a large earthquake is closely preceded in space and time by a smaller one, or series of smaller ones, commonly known as foreshocks. There is disagreement, however, over whether foreshocks actually trigger their main shocks or are simply by-products of the main shock nucleation process. Support for the former view includes *Kagan and Knopoff* [1981], *Abercrombie and Mori* [1994], *Mori* [1996], *Michael and Jones*

[1998], and *Kilb and Gomberg* [1999], while support for the latter includes *Dodge et al.* [1995], *Dodge et al.* [1996], and *Hurukawa* [1998].

[6] We first define what we mean by “aftershocks.” We then provide evidence from earthquake statistics that foreshocks trigger their main shocks and that, in general, the magnitude of a triggered earthquake is independent of the magnitude of its trigger. Hence it is possible that small Landers aftershocks played an important role in the triggering of the Hector Mine earthquake.

### 2.1. Definition of Aftershocks

[7] It has long been recognized that earthquakes cluster in time on a scale of seconds, days, and years. After a large earthquake, this clustering is particularly pronounced as many other earthquakes follow in a short time period. The

earthquake that initiates such activity is known as a main shock, and the clustered earthquakes that follow are known as aftershocks. The rate of aftershock occurrence follows the modified Omori law [Utsu, 1961], a robust empirical relationship given as

$$R = \frac{A}{(c + t)^p},$$

where  $R$  is the rate of aftershocks and  $t$  is time after the main shock,  $A$  is the productivity constant,  $c$  is a constant with units of time which is important for fitting the aftershock rate, and  $p$  is the decay rate constant, typically slightly larger than one. Aftershocks also show spatial clustering around the main shock fault.

[8] Apart from their distinct clustering behavior, aftershocks appear identical to other earthquakes. Hence we understand an aftershock as any earthquake that would have occurred at a later time, or not at all, if it had not been influenced by a previous earthquake. For the purposes of this study, the essential quality of aftershocks is that they occur in distinct sequences of earthquakes that adhere to Omori's law. We also define a main shock as any earthquake that initiates such a sequence. Note that a single earthquake may be both a main shock and an aftershock.

[9] For our modeling we assume that complex earthquake interactions can be adequately treated by presuming that a main shock can produce only two types of aftershocks. One type is direct aftershocks, which are triggered solely by a given main shock (in the sense that their timing and size are independent of stress perturbations from other earthquakes). Direct aftershocks can be adequately described by an Omori's law that begins at the time of the given main shock. The other type is secondary aftershocks, which occur on faults that have been so significantly stressed by a previous aftershock that the Omori's law which best describes them begins at the time of this triggering aftershock rather than at the time of the original main shock. Secondary aftershocks may be triggered by either direct aftershocks or other secondary aftershocks and may be significantly composed of earthquakes that would not have been triggered by the stress changes of the original main shock. In our modeling we will create distinct direct and secondary aftershocks by determining the timing of each aftershock from a single earlier event. We will also use the same parameters and the same equation (the modified Omori law) to generate both direct and secondary aftershocks. Doing so significantly reduces the number of free parameters in the problem and will be further justified below.

[10] In accordance with *Michael and Jones* [1998] we put no restrictions on the relative sizes of the main shock and aftershock, although we will specifically use the term foreshock to describe a main shock that is smaller than its aftershock. This is consistent with our hypothesis that small earthquakes are capable of triggering larger ones, which we will demonstrate in section 2.2.

## 2.2. Main Shock and Aftershock Magnitude

[11] The simplest model that allows small earthquakes to trigger large ones is that the nucleation process of earthquakes of all magnitudes is scale invariant, as has been

proposed by *Kagan and Knopoff* [1981], *Abercrombie and Mori* [1994], *Mori and Kanamori* [1996], *Kilb and Gomberg* [1999], and others and has been found in physically based theoretical models of earthquake sequences [Lapusta *et al.*, 2000; N. Lapusta and J. R. Rice, Nucleation and early seismic propagation of small and large events in a crustal earthquake model, submitted to *Journal of Geophysical Research*, 2002, hereinafter referred to as Lapusta and Rice, submitted manuscript, 2002]. This means that the fault area that must be stressed to start an event is the same for all earthquakes (in a given normal stress and lithological regime), and therefore must be the same size as, or smaller than, the smallest earthquake possible. Once an earthquake starts, the stress changes generated by the propagating rupture are far greater than the typical static stress transfer; hence it is reasonable to believe that dynamic stressing and fault geometry [Harris and Day, 1993] in combination with substantial fluctuations in the prestress distribution (Lapusta and Rice, submitted manuscript, 2002) are the most important factors in its continued propagation and final extent. Under these assumptions, the size of the triggering earthquake has little or no control over the final size of the earthquake triggered; or, stated conversely, the magnitude of an aftershock is essentially independent of the size of the main shock that triggered it.

[12] If main shock magnitude does not determine aftershock magnitude, we can assume that the size of any given aftershock is chosen randomly from the Gutenberg-Richter magnitude-frequency distribution [Gutenberg and Richter, 1944]. This distribution is a robust empirical description of magnitudes in regional earthquake populations and is given by

$$\log_{10}[N(m)] = a - bm,$$

where  $N(m)$  is the number of earthquakes greater than or equal to magnitude  $m$  and  $b$  is a constant which is generally close to unity. The constant  $a$  is slightly less than the magnitude of the largest earthquake in the population for time periods long enough for a significant amount of seismicity to accumulate but not longer than the average repeat time of the largest earthquake possible.

[13] If the smallest earthquake possible has a magnitude of  $M_{\min}$ , the Gutenberg-Richter relationship predicts that the total number of earthquakes in the population is equal to  $10^{a-bM_{\min}}$ . Thus the probability that a randomly chosen earthquake is greater than or equal to some magnitude  $m$  is given by

$$P(m) = \frac{10^{a-bm}}{10^{a-bM_{\min}}} = 10^{b(M_{\min}-m)}.$$

Therefore, as pointed out by *Reasenber and Jones* [1989], in this model  $N_A(m_1, m_2)$ , the number of aftershocks produced by a main shock of  $m_1$  that we expect to be greater than or equal to  $m_2$ , is given by

$$N_A(m_1, m_2) = N_A(m_1, M_{\min})P(m_2) = N_A(m_1, M_{\min})10^{b(M_{\min}-m_2)}$$

Where  $N_A(m_1, M_{\min})$  is the total number of aftershocks produced by a main shock of magnitude  $m_1$  and  $P(m_2)$  is the

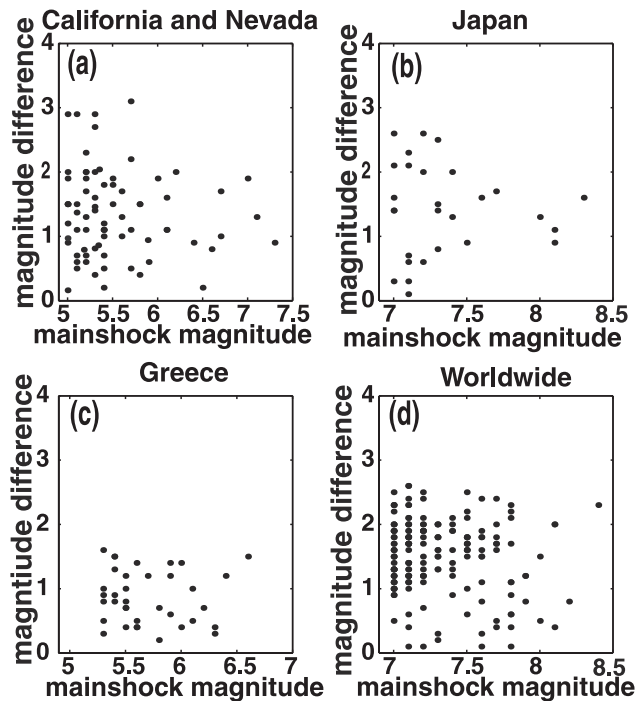


**Figure 2.** Main shock magnitude plotted against the difference between the main shock and largest aftershock magnitude for (a) our California-Nevada data set, (b) Japanese earthquakes from *Utsu* [1961], (c) Greek earthquakes from *Drakatos and Latoussakis* [2001], and (d) large worldwide earthquakes from *Tsapanos* [1990]. All data sets satisfy Båth's law that states that the difference in magnitude between the main shock and the largest aftershock is independent of main shock size. (The squared correlations are 0.019, 0.013, 0.002, and 0.015, respectively.) There are no negative  $y$  axis values in accordance with the definition of aftershocks used in the other studies.

probability that a random aftershock will have a magnitude  $\geq m_2$ . We can use this expression to predict how many large aftershocks should follow small main shocks. We will then compare this prediction to observed foreshock statistics to test our model. In section 2.3 we use the empirical relationship known as Båth's law [*Richter*, 1958; *Båth*, 1965] to solve for  $N_A(m_1, M_{\min})$ , and we obtain an explicit expression for  $N_A(m_1, m_2)$ .

### 2.3. Using Båth's Law to Calculate Aftershock Production

[14] Båth's law states that the average difference in size between a main shock and its largest aftershock is 1.2 magnitude units, regardless of main shock magnitude [*Richter*, 1958; *Båth*, 1965]. We verify this empirical relationship using aftershock data from *Utsu* [1961], *Tsapanos* [1990], and *Drakatos and Latoussakis* [2001] and a data set of our own based on California and Nevada earthquakes from the Council of the National Seismic System (CNSS) catalog. This additional data set consists of 79  $M \geq 5$  earthquakes that occurred between 1975 and 2000 and their aftershocks (Figure 2). We exclude earthquakes that occurred in the Mammoth Lakes volcanic caldera, where seismicity is influenced by magma, as well as  $M \geq 5$

earthquakes that were so close in time and space to a previous large earthquake that their independent aftershocks could not be determined. We identify as aftershocks all  $M \geq 2$  earthquakes that occurred within 1 month of an  $M \geq 5$  main shock and within the area that contained spatially clustered seismicity about the main shock epicenter, by visual inspection. The aftershocks thus identified were generally located within two to three fault lengths of the main shock epicenter.

[15] In all of the studied data sets we find that the difference in magnitude between the main shock and the largest aftershock is independent of main shock magnitude, although the average value of the difference varies between 1.0 and 1.4 for the different data sets (for California-Nevada the difference is  $1.28 \pm 0.19$ ). Thus we find that Båth's law is generally valid, meaning that on average an increase in the magnitude of a main shock from  $m_1$  to  $m_1 + 1$  corresponds to a matching increase in the magnitude of the largest aftershock from  $m_a$  to  $m_a + 1$ . We show in section 2.2, however, that  $P(m_2)$ , the probability of a random earthquake having  $M \geq m_2$ , is equal to  $10^{b(M_{\min} - m_2)}$ , or  $P(m_a + 1) = (1/10^b) P(m_a)$ . Therefore to satisfy both Båth's law and the hypothesis that the magnitude of each aftershock is chosen at random, the decreased probability of any particular aftershock having a magnitude 1.2 units below the main shock as main shock magnitude increases must be offset with an increased number of aftershocks. That is

$$N_A(m_1 + 1, M_{\min}) = 10^b N_A(m_1, M_{\min}),$$

and so we conclude that  $N_A(m_1, M_{\min})$  varies as a power of  $10^b$  with main shock magnitude

$$N_A(m_1, M_{\min}) = 10^{b(m_1 - d)}.$$

The constant  $d$  depends on the time and area chosen for counting aftershocks, and presumably on the tectonic region. Since  $M_{\min}$  is a constant, we can rewrite  $d = C - M_{\min}$  (where  $C$  is a constant) and substitute  $N_A(m_1, M_{\min})$  back into our expression to solve for  $N_A(m_1, m_2)$ :

$$\begin{aligned} N_A(m_1, m_2) &= N_A(m_1, M_{\min}) P(m_2) = 10^{b(m_1 - C + M_{\min})} 10^{b(M_{\min} - m_2)} \\ &= 10^{b(m_1 - C - m_2)}. \end{aligned}$$

This result agrees with the theoretical results of *Reasenber and Jones* [1989] and *Kagan* [1991] and the empirical observations of *Yamanaka and Shimazaki* [1990]. *Michael and Jones* [1998] have also shown the converse, that assuming aftershock production varies as  $10^{bm_1 - d}$  reproduces Båth's law. *Kurimoto* [1959] and *Vere-Jones* [1969] also worked on the hypothesis that Båth's law can be reproduced if the magnitude of each aftershock is chosen at random.

### 2.4. Testing Foreshock Predictions

[16] Our results in section 2.3 indicate that aftershock productivity varies as  $10^{bm}$ ; conversely, we know from the Gutenberg-Richter relationship that earthquake frequency varies as  $10^{-bm}$ . So changes in the number of aftershocks produced per main shock is balanced by change in the number of main shocks, and the total number of aftershocks

produced by the total number of earthquakes in each unit magnitude level should be the same. A similar conclusion was reached by *Michael and Jones* [1998]. *Hanks* [1992] used an analogous argument to demonstrate that small and large earthquakes are equally important in stress redistribution along major fault zones.

[17] To test whether the percentage of aftershocks produced by each magnitude range is indeed a constant, we investigate the California-Nevada  $M \geq 5$  earthquake population. If our model is correct, we would expect that the percentage of this population that has  $M 2-3$  foreshocks, for example, is the same as the percentage of the population that has  $M 4-5$  foreshocks, and the same as the percentage that occurs as aftershocks of  $M 7-8$  main shocks. Conversely, if foreshocks have no triggering ability but rather are triggered by a fault preparing for a larger earthquake or occur by chance, we would not expect to find any particular link between foreshock statistics and the number of  $M \geq 5$  aftershocks produced by larger earthquakes. We would also not expect the magnitudes of foreshocks to be evenly distributed. Rather, foreshocks should be predominantly small, since small earthquakes dominate earthquake catalogs.

[18] Unfortunately, however, the aftershocks of earthquakes of all magnitudes are not equally observable. The aftershocks of an  $M 7$  earthquake can generally be counted quite easily, for example, but the aftershocks of an  $M 2$  earthquake may be difficult to isolate if the  $M 2$  happens to occur within the early aftershock sequence of the  $M 7$ . We solve this problem by measuring the percentage of aftershocks triggered by each magnitude range from a data subset that excludes early aftershocks of larger main shocks. As long as the data subset used still contains a Gutenberg-Richter distribution of magnitudes and has the same  $b$  value as the data excluded, this method will not bias our results as the ratio of potential main shocks to potential aftershocks will remain constant.

[19] The data set we chose is the 1975–1995 California-Nevada earthquake data set of *Abercrombie and Mori* [1996], which corresponds geographically with our region of interest for the Hector Mine earthquake. *Abercrombie and Mori* [1996] identified as foreshocks  $2 \leq M < 5$  earthquakes that occurred within 30 days and 5 km of an  $M \geq 5$  main shock. They eliminated from their data the Mammoth Lakes volcanic region (where moving magma causes complications by adding variable stresses to the system) and regions in which the recording completeness level was above  $M 2.0$ . From the remaining data they identified 59  $M \geq 5$  earthquakes that were not obvious aftershocks of other  $M \geq 5$  earthquakes. Eight of them had largest foreshocks of  $M 2-3$ , ten had largest foreshocks of  $M 3-4$ , and eight had largest foreshocks of  $M 4-5$ . We examine the 78 remaining  $M \geq 5$  earthquakes in the data set and find that 52 of them occurred as 30-day aftershocks of other  $M \geq 5$  earthquakes, with 15 following  $M 7-8$  earthquakes, 22 following  $M 6-7$  earthquakes, and 16 following  $M 5-6$  earthquakes. We inspected the remaining 26 earthquakes for foreshocks. Many of these earthquakes were aftershocks of  $M \geq 5$  earthquakes that followed the main shock by two months to several years. We found that the aftershock sequences had quieted down enough by this point that foreshocks could be identified if we limited ourselves to 24 hours before the main shock (a time period

in which *Abercrombie and Mori* [1996] found that most foreshocks occur in any case). Doing so, we found 2 additional earthquakes with  $M 2-3$  foreshocks, 2 with  $M 3-4$  foreshocks, and 3 with  $M 4-5$  foreshocks.

[20] We can now calculate the percentages of the relevant  $M \geq 5$  earthquake populations that follow main shocks of different magnitude ranges. We find that  $15/137 = 11\%$  of  $M \geq 5$  earthquakes follow  $M 7-8$  main shocks,  $22/122 = 18\%$  follow  $M 6-7$ ,  $16/100 = 16\%$  follow  $M 5-6$ ,  $11/84 = 13\%$  follow  $M 4-5$ ,  $12/73 = 16\%$  follow  $M 3-4$ , and  $10/62 = 16\%$  follow  $M 2-3$ . The average percentage for all the magnitude levels is 15%, and using binomial probability, we estimate that given the sample sizes, the variation from this average at the 95% confidence level should go from  $\pm 6\%$  for the  $M 7-8$  main shocks to  $\pm 9\%$  for the  $M 2-3$  foreshocks. All of the values measured are within these limits. Therefore, we can conclude that the data is statistically consistent with our prediction that the percentage of  $M \geq 5$  earthquakes occurring as aftershocks of each magnitude range should be constant. Thus the data are consistent with our hypothesis that main shock and aftershock magnitude are independent, and that foreshocks are simply small main shocks with large aftershocks.

[21] As additional support, *Reasenber* [1999] notes in a survey of seven different foreshock studies that foreshocks are always evenly distributed with magnitude. The percentage of main shocks that derive foreshocks from a single magnitude unit range appears to average worldwide at 13.6%, with a range between 12% and 17% [*Reasenber*, 1999]. Our central assumption that aftershock and main shock magnitudes are independent also means that the magnitudes of foreshocks and their corresponding main shocks should not be correlated. This has been observed by *Abercrombie and Mori* [1996] and by a number of other authors including *Jones and Molnar* [1979], *Jones* [1984], *Agnew and Jones* [1991], and *Reasenber* [1999].

[22] In general, any single small main shock is unlikely to have a large aftershock simply because it has few aftershocks. There are many small main shocks, however, and taken as a group they are just as likely to produce large aftershocks as the smaller number of large main shocks are. Therefore we conclude that it is possible that one of the numerous small aftershocks of the Landers earthquake was the direct trigger of the Hector Mine earthquake. We will next demonstrate that this scenario is not only possible, but likely.

### 3. Evidence That the Hector Mine Earthquake Was Triggered by an Aftershock of the Landers Earthquake

#### 3.1. Observational Evidence

[23] It has long been recognized that aftershocks have their own aftershocks, often referred to as “secondary aftershocks” [*Richter*, 1958]. It is often impossible to isolate secondary aftershocks from the rest of the sequence, however, unless they are in some way temporally or spatially isolated.

[24] Spatial and temporal isolations both indicate that most Landers earthquake aftershocks in the Hector Mine earthquake epicentral region were secondary, triggered by the 5 July 1992  $M 5.4$  Pisgah aftershock and its aftershocks.

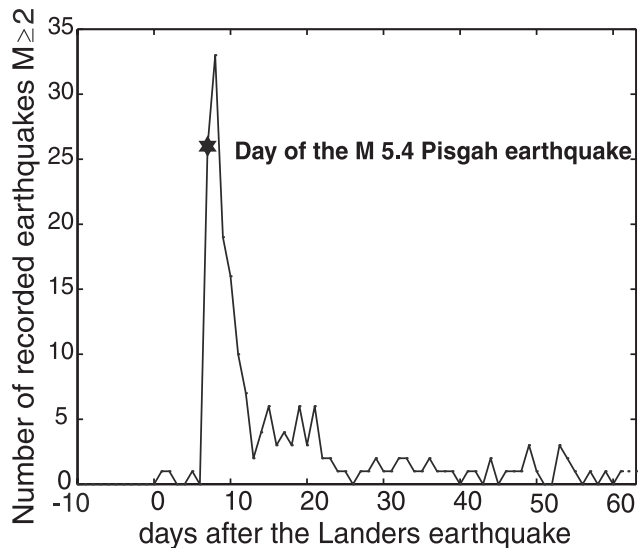


**Figure 3.** Seismicity in the Hector Cluster region (see Figure 1) increased after the Landers earthquake but increased much more after the  $M_W$  5.4 Pisgah earthquake 7 days later. This suggests that most of the aftershocks in the Hector Mine cluster region were direct or secondary aftershocks of the Pisgah earthquake and only secondary aftershocks of the Landers earthquake.

In the 7 days following the Landers earthquake, the seismicity rate in a  $26 \text{ km} \times 17 \text{ km}$  region around the future Hector Mine epicenter (box in Figure 1) increased from an extremely low level ( $1.2 M \geq 2$  earthquakes/yr) to an average of  $4.3 M \geq 2$  earthquakes/d. In the 7 days after the Pisgah earthquake, however, the rate quadrupled to an average of  $17.1 M \geq 2$  earthquakes/d (Figure 3) and a distinct spatial cluster formed (Figure 1). This indicates that even though the Pisgah earthquake was nearly two magnitude units smaller than the Landers earthquake, its location within several kilometers of the future Hector Mine earthquake hypocenter made it locally a more important stressor [also see *Harris and Simpson, 2002*]. Indeed, because earthquakes of all magnitudes have roughly comparable stress drops [e.g., *Kanamori and Anderson, 1975; Abercrombie, 1995*] and thus produce comparable static stress changes in the near field, a small earthquake that is close can produce higher static stress changes than a larger earthquake that is farther away.

[25] Perhaps even more important for the triggering of the Hector Mine earthquake than the Pisgah earthquake, however, were  $M$  4.3 and  $M$  4.1 earthquakes that occurred within 2 km of the Hector Mine epicenter in August and October 1996, respectively. These earthquakes triggered a strong local seismicity response (Figure 4). Another sharp increase in near-epicentral seismicity commenced with the beginning of the Hector Mine foreshock sequence on 15 October 1999 (Figure 4).

[26] Since the Pisgah earthquake also had apparent foreshocks, one possible triggering scenario for the Hector Mine earthquake is the Landers earthquake  $\rightarrow$  Pisgah foreshocks  $\rightarrow$  Pisgah earthquake  $\rightarrow$   $M$  4.3  $\rightarrow$   $M$  4.1  $\rightarrow$  Hector Mine foreshocks  $\rightarrow$  Hector Mine earthquake. However, this or any other detailed scenario is impossible to prove. Attempts

at calculating static, dynamic, or other stress changes produced by the earthquakes in the potential chain would be compromised because the 1996  $M$  4 earthquakes, Hector Mine foreshocks, and Hector Mine epicenter are so close to one another that small errors in location and focal parameters would significantly alter the results. In addition,  $M$  3,  $M$  2, and smaller earthquakes may have been critical links in the triggering chain. Finally, it is unclear whether the Big Bear aftershock ( $M_W$  6.2–6.5 [*Dziewonski et al., 1993; Hauksson, 1994*]), whose own aftershock lineations point toward the Hector Mine cluster (Figure 1), should be included as part of the calculation. Instead of investigating any particular stress transfer path, then, we use Monte Carlo simulations of the Landers aftershock sequence to estimate the probability that if the Hector Mine earthquake was an aftershock of the Landers earthquake, it was a secondary rather than a direct aftershock.

### 3.2. Statistical Evidence

[27] If the Hector Mine earthquake was an aftershock of the Landers earthquake, the probability that it was a secondary aftershock is equal to the percentage of seventh-year Landers aftershocks that were secondary. There is no easy way to calculate this percentage analytically, so we estimate the percentage with Monte Carlo simulations of the Landers aftershock sequence. In our Monte Carlo trials we simulate only the time and the magnitudes of each after-

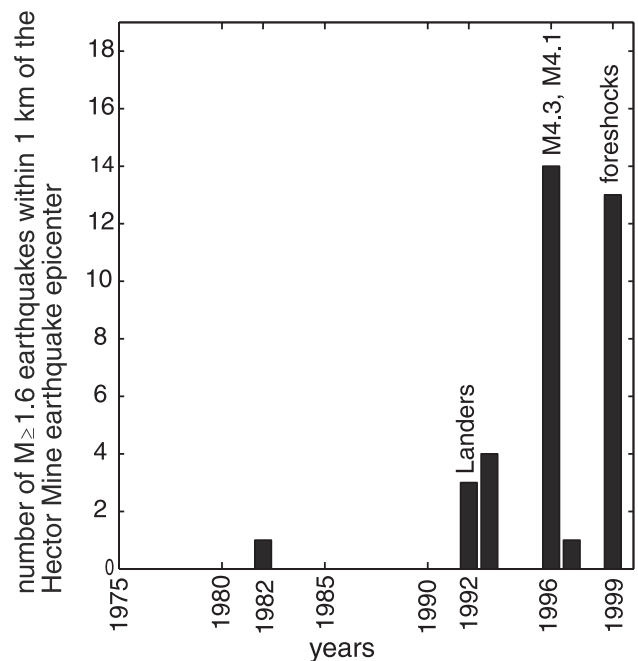


**Figure 4.** Number of earthquakes ( $M \geq 1.6$ ) within 1 km of the Hector Mine earthquake epicenter with time. (On average seismicity is complete down to  $M$  1.6 in the region.) Each bar represents 1 year. Before the Landers earthquake the area was seismically quiet. After the Landers main shock in 1992 a few earthquakes occurred, but the largest seismicity increases occurred after a nearby  $M$  4.3 and  $M$  4.1 in 1996 and after the beginning of the Hector Mine foreshock sequence in 1999.

shock. The spatial dimension, which is considerably more complex, is not dealt with explicitly.

### 3.2.1. Monte Carlo Simulations

[28] To generate aftershock magnitudes and times in our Monte Carlo simulations, we use the inverse transform method [e.g., *Rubinstein*, 1981] for choosing sample values from an arbitrary probability distribution. The key observation is that if  $G_X(x)$  is the cumulative distribution function (CDF) of a variable  $x$ , then

$$G_X(x) = P\{X \leq x\},$$

where  $P\{X \leq x\}$  is the probability that a randomly chosen value from the population of  $X$  will be  $\leq x$  and thus must be uniformly distributed between 0 and 1. This allows us to set  $G_X(x)$  equal to  $r$ , where  $r$  is a uniform random number  $0 < r \leq 1$ , and then invert the equation to obtain sample values for  $x$  in terms of  $r$ :

$$x = G_X^{-1}(r).$$

Note that we can also write

$$1 - G_X(x) = P\{X \geq x\} = r.$$

This second form is more convenient for our purposes. We use this equation in our procedure, which consists of three steps:

1. We determine the magnitude of each aftershock by using the inverse transform method to select random magnitudes from the Gutenberg-Richter distribution

$$1 - G_M(m) = 10^{b(M_{\min} - m)} = P\{M \geq m\} = r$$

to obtain

$$m = M_{\min} - \log_{10}(r)/b.$$

2. We select the timing of each aftershock from the modified Omori law distribution by calculating a CDF from the nonstationary Poissonian function based on the modified Omori law. The regular Poissonian function describes random processes that occur at a steady rate with time, whereas the nonstationary Poissonian describes random processes whose rate changes with time. The nonstationary Poissonian is therefore appropriate for modeling aftershock sequences [*Toda et al.*, 1998]. Our equation is

$$1 - G_{T_2}(t_2) = \exp\left(-\int_{t_1}^{t_2} A(t+c)^{-p} dt\right) = P\{T_2 \geq t_2\} = r,$$

where  $t_1$  is the time of the last aftershock and  $t_2$  is the time of the next aftershock. Solving the integral, inverting, and simplifying we obtain

If  $p = 1$

$$t_2 = r^{-1/A} t_1 + c(r^{-1/A} - 1).$$

If  $p \cong 1$

$$t_2 = (t_1 + c)^{1-p} - (1-p) \left[ \frac{\ln(r)}{A} \right]^{1/(1-p)} - c.$$

With the restriction that if  $p > 1$  it is required that

$$r > e^{A/(1-p)}(t_1 + c)^{1-p}.$$

If  $r$  is less than this value, no more aftershocks will occur.

3. The aftershock productivity of each earthquake in the sequence is determined by setting the  $A$  parameter in the modified Omori law equal to  $A_D 10^{bM}$ , where  $M$  is the magnitude of the main shock in question and  $A_D$  is the productivity constant of the direct aftershock sequence.

### 3.2.2. Parameter Fitting for the Monte Carlo Simulations

[29] The parameters needed for the model simulations are  $A_D$ ,  $c$ , and  $p$  for the modified Omori law and  $b$  and  $M_{\min}$  for the Gutenberg-Richter law. From a linear regression of all of the Landers aftershock data (which are complete down to  $M 4$ ) we get a  $b$  value of  $1.02 \pm 0.09$ ; we chose a  $b$  value of unity for the simulation. We choose 0 for  $M_{\min}$ , since it has been documented that shear-slip earthquakes with stress drops comparable to those of larger earthquakes can be at least as small as  $M = 0$  [*Abercrombie*, 1995]. It has also been shown in mines that the smallest shear-rupture earthquakes are  $M \approx 0$  [*Richardson and Jordan*, 2002].

[30] For the Omori parameters, it is important to emphasize that we seek the parameters that describe only the direct sequence of aftershocks that follows each main shock. These are not the same parameters that would produce a best fit curve to the observed sequence made up of both direct and secondary aftershocks, which has a higher activity level and slower decay rate. We use forward modeling to solve for the Omori parameters, minimizing the least squares residual between the model and observations for how many  $M_W \geq 2$  aftershocks occurred on each of the first 5 days of the Landers aftershock sequence and, cumulatively, over the first 7 years. This is done by choosing one parameter combination, running 300 simulations, comparing the average of the simulation results with the observed aftershock sequence, adjusting the parameters, performing another set of runs, and so on.

[31] To calculate observed daily earthquake counts for the Landers aftershock sequence, we first consider all of the seismicity recorded in the composite Council of the National Seismic System (CNSS) catalog in the geographical region  $33.64^\circ\text{N}$  to  $35.39^\circ\text{N}$  and  $-117.39^\circ\text{W}$  to  $-115.57^\circ\text{W}$ . This region was chosen because it contains visibly clustered Landers aftershocks. Choosing these bounds will exclude some aftershocks that occurred quite far from the epicenter, which will cause us to underestimate the activity parameter  $A_D$ . Thus we will slightly under predict how many Landers aftershocks were secondary.

[32] We then convert the CNSS catalog magnitudes that are  $M_c$ , to  $M_W$ .  $M_c$  is essentially equal to  $M_L$ , so we use straight-line approximations to the *Hanks and Boore* [1984] curve for conversion from  $M_L$  to  $M_0$  (in dyn cm):

$$\begin{aligned} \log(M_0) &= M_L + 17.1; & M_L < 2; \\ \log(M_0) &= 1.37M_L + 16.46; & 3.8 > M_L \geq 2; \\ \log(M_0) &= 1.5M_L + 16.1; & 6 > M_L \geq 3.8; \end{aligned}$$

and then convert from  $M_0$  to  $M_W$  using [*Kanamori*, 1977]

$$M_W = \log(M_0)/1.5 - 10.73.$$

We then check for catalog completeness down to  $M_W 2$  for the beginning of the Landers aftershock sequence, when the high activity rate caused some small earthquakes to be unrecorded. We find that the Landers sequence can only be considered complete down to  $M_W 2$  after the first 10 days. We estimate new aftershock counts for the first 10 days by first using the Gutenberg-Richter relationship to estimate the magnitude to which the sequence was complete. To be safe, we add 0.1 to this magnitude to get a “completeness” magnitude  $m_c$ , and then we count the number of earthquakes  $M \geq m_c$ . We then use the Gutenberg-Richter relationship with  $b = 1$  and  $a = m_c - 0.05$  to estimate the number of earthquakes  $M_W \geq 2$ . The factor of 0.05 is subtracted because rounding in the CNSS catalog means that magnitudes reported as  $m_c$  may actually be as small as  $m_c - 0.05$ .

[33] Finally, we need to account for the fact that not all of the earthquakes occurring after the Landers earthquake in the region we have chosen are actually Landers aftershocks. Our catalog also includes aftershocks of the 23 April 1992  $M_W 6.2$  Joshua Tree earthquake and independent earthquakes, often referred to as “background” seismicity. We estimate the effect of the Joshua Tree earthquake by fitting the first 66 (pre-Landers earthquake) days of the Joshua Tree aftershock sequence with our model and then using Monte Carlo simulations to project how many more aftershocks would have occurred over the next 7 years. We estimate the background seismicity rate from the CNSS earthquake catalog from the time period June 1980 to December 1985, when there were no  $M_W \geq 5$  earthquakes creating peaks in the seismicity rate. We find that at the time of the Landers earthquake, the Joshua Tree sequence and the background rate combined were contributing two to four  $M \geq 2$  earthquakes per day. Since there were hundreds of earthquakes per day at the beginning of the Landers aftershock sequence, there is no need to change our early aftershock count. Over the 7 years between the Landers and Hector Mine earthquakes, however, we estimate that the Joshua Tree sequence contributed about 1200 earthquakes and the background rate about 2690 earthquakes. We subtract this from our 7-year total  $M \geq 2$  Landers aftershock count of 25,810 before fitting the Omori parameters.

[34] We also note that the number of aftershocks per day in a sequence is sensitive not only to the Omori parameters but also to the largest magnitude aftershock to occur in the sequence (Figure 5). Therefore, to make our simulated sequences as close to the actual Landers aftershock sequence as possible, we use only those sequences that contain first-day aftershocks in the magnitude range of  $M_W 6.15$ – $6.55$ . This is the range estimated for the Big Bear aftershock, which occurred on the first day of the Landers sequence and was the largest aftershock to occur before the Hector Mine earthquake. In accordance with the data, we also do not allow production of any aftershock larger than  $M_W 6.55$  before the time of the Hector Mine earthquake. Allowing larger aftershocks to occur would increase the average number of aftershocks per day produced with the same set of Omori parameters, causing incorrect parameters to be solved for.

[35] We find that all of the Omori parameter combinations that fit the 7-year cumulative Landers aftershock count produce the same percentage of secondary aftershocks in

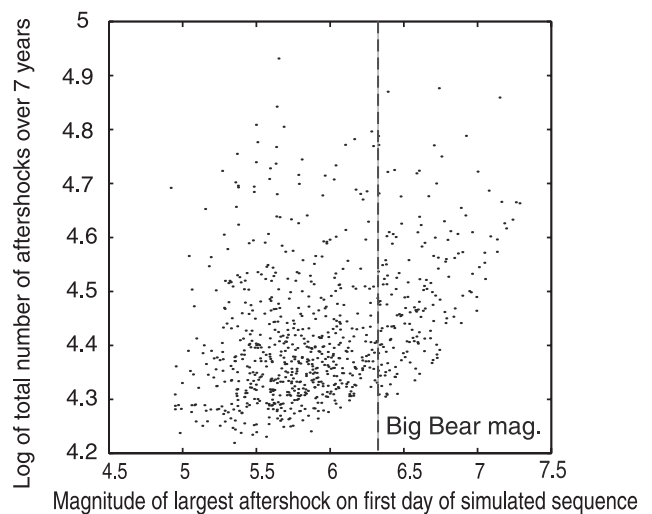


**Figure 5.** The total number of aftershocks over 7 years of the simulated aftershock sequences varies significantly with the magnitude of the largest aftershock on the first day of the sequence. Thus, to most closely reproduce the actual Landers aftershock sequence with our simulations, we only use simulated sequences that have first-day aftershocks in the magnitude range of the Big Bear aftershock, the largest first-day aftershock in the Landers earthquake sequence.

the seventh year. Fitting the cumulative aftershock total is therefore sufficient to give us the percentage of aftershocks that are secondary. We also fit the first 5 days of the aftershock sequence, however, to get values for  $A_D$ ,  $p$ , and  $c$ . Having these values allows us to compare the shapes of the modeled and observed sequences to check the validity of our model assumptions. An average of model runs with the best fit parameters of  $A_D = 0.0058 \text{ day}^{p-1}$ ,  $p = 1.25$ , and  $c = 0.08 \text{ day}$  is shown with the Landers aftershock sequence in Figure 6.

[36] In addition to solving for the best fit parameters, we also hold  $p$  and  $c$  fixed and vary  $A_D$  to solve for the smallest and largest activity constants that still satisfy the 7-year cumulative aftershock count of the Landers sequence at least 2% of the time. Having these values allows us to determine complete error bars. We find that the minimum and maximum  $A_D$  values are 0.00535 and 0.00630  $\text{day}^{p-1}$ , respectively. We do not need to vary all three Omori parameters because as noted above, the percentage of aftershocks that are secondary in the seventh year will be the same for any parameter combination that produces the correct total number of aftershocks over 7 years.

### 3.2.3. Simulation results

[37] After solving for the parameters, we run an additional 1500 simulations of the Landers aftershock sequence with the best fit parameters and the restriction that no pre-Hector Mine aftershock can be larger than the  $M_W 6.15$ – $6.55$  Big Bear earthquake. This gives us 300 sequences that attained a first-day aftershock of similar magnitude to the Big Bear aftershock and are therefore similar enough to the Landers aftershock sequence. If we do not make this restriction, allowing aftershocks to be any magnitude up to the size of the main shock, we get slightly larger error

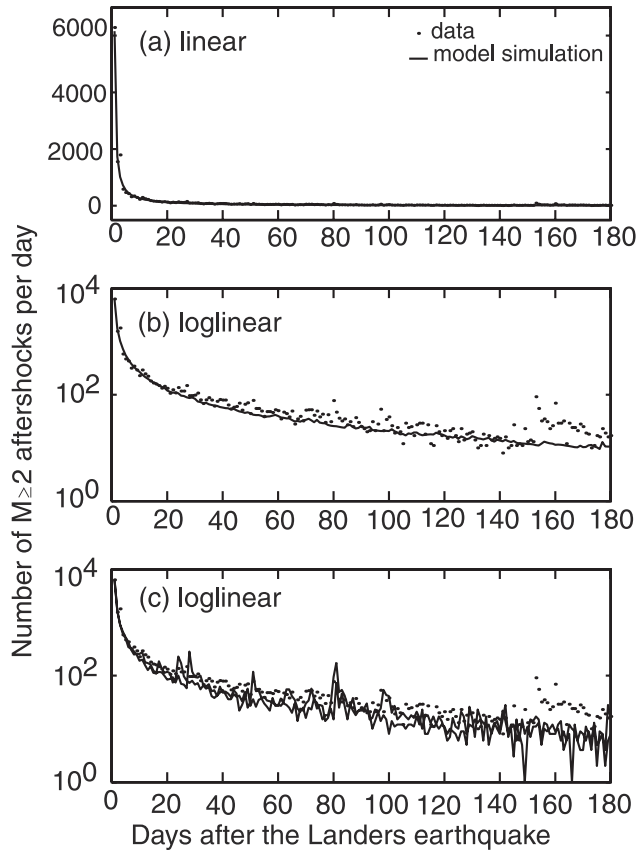


**Figure 6.** Results of the Monte Carlo simulations with best fit parameters of  $A_D = 0.0058 \text{ day}^{p-1}$ ,  $p = 1.25$ , and  $c = 0.08$  days, plotted against the observed Landers aftershock time series. The observed time series consists of all  $M \geq 2$  earthquakes within the geographical bounds  $33.64^\circ\text{N}$  to  $35.39^\circ\text{N}$  and  $-117.39^\circ\text{W}$  to  $-115.57^\circ\text{W}$ , with an estimated number of additional aftershocks added to the first ten days to make up for incomplete recording of small shocks. The model parameters are fit to this data minus the number of non-Landers aftershocks (Joshua Tree aftershocks plus background events) that we estimate to have occurred over this area and time period. Hence the model is expected to be slightly lower than the data. The increase in the data starting around day 150 is due to  $M 5.4$  and  $M 5.2$  aftershocks. (a) Average daily aftershock counts from 300 runs of the model plotted against the data on a linear scale. (b) Average daily aftershock counts from 300 runs of the model plotted against the data on a log linear scale. (c) Two arbitrarily selected runs of the model plotted against the data on a log linear scale to demonstrate that the model and data display similar amounts of variability.

bars on our final answer and a higher mean probability that Hector Mine was a secondary aftershock (Figure 7).

[38] Our 300 simulated sequences are sufficient to produce a stable mean and 98% confidence intervals for the percentage of 7-year Landers aftershocks that were secondary. Because the data are not normally distributed (Figure 8), we calculate the mean and 98% confidence intervals by performing 1000 bootstrap resamplings of the data. We find that in the seventh year of the model sequences on average

82.5% of the aftershocks are secondary with a 98% confidence range from 69.7% to 95%. Hence, on the basis that the Hector Mine earthquake occurred 7 years after the Landers earthquake, we can assign an 82.5% probability that it was a secondary, rather than a direct, aftershock of Landers.

[39] We can refine this probability with the observation that the aftershock immediately preceding the Hector Mine earthquake in the Landers aftershock sequence happened only 0.29 day beforehand. Our simulations show that the aftershock rate had dropped low enough by the seventh year that secondary aftershocks were significantly more likely to occur within 0.29 day of the previous aftershock in the sequence than direct aftershocks were. Specifically, if we use  $T$  to represent a time interval between consecutive earthquakes that is 0.29 day or shorter, and  $S$  to stand for an earthquake that is a secondary aftershock, we find from our simulations that  $P(T | S) = 0.305$  and  $P(T) = 0.291$ . Using conditional probability, this increases our probability that the Hector Mine earthquake was a secondary aftershock from 82.5% to 85%.

[40] In fact, if we could take the spatial dimension into account, we would probably find that this probability is

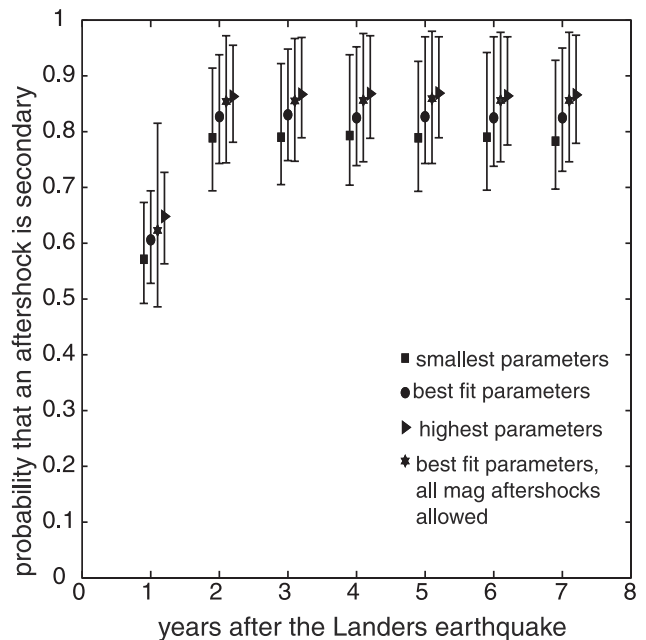


**Figure 7.** The probability that a random aftershock in the Landers aftershock sequence is secondary, by year after the main shock, plotted with 98% error bars. Circles show results for the best fit parameters ( $A_D = 0.0058 \text{ day}^{p-1}$ ,  $p = 1.25$ ,  $c = 0.08$  day) with the first day aftershock limited to the Big Bear aftershock range and no aftershock allowed to be larger than Big Bear. Stars show results for the best fit parameters with the sole limitation that no aftershock can be larger than the main shock. Triangles show results for the highest activity parameter ( $A_D = 0.00630 \text{ day}^{p-1}$ ), and squares show results for the lowest activity parameter ( $A_D = 0.00535 \text{ day}^{p-1}$ ) that can still fit a Landers earthquake-like sequence at least 2% of the time. The high and low fit parameter simulations are both done with aftershock magnitude limitations as described above. Symbols are offset for clarity.

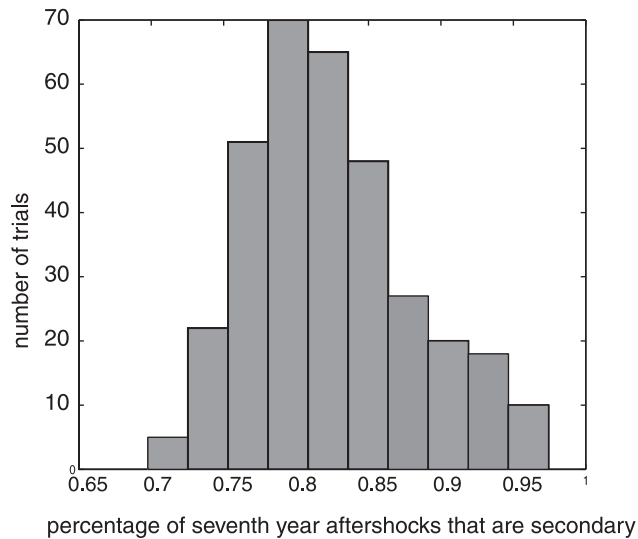


**Figure 8.** Distribution of Monte Carlo simulation results for the percentage of aftershocks occurring in the seventh year that are secondary aftershocks. Since the data are not normally distributed, we use bootstrapping to estimate the mean and 98% confidence intervals.

much higher. In addition to occurring just hours before the Hector Mine earthquake, the previous recorded earthquake, and the nine before it, also occurred within 2 km of the Hector Mine epicenter. These earthquakes all satisfy the *Abercrombie and Mori* [1996] criterion for foreshocks described earlier.

## 4. Discussion

### 4.1. Model Assumptions

#### 4.1.1. Model Parameters

[41] One source of uncertainty in our model is that we do not have a precise value for  $M_{\min}$ , the magnitude of the smallest earthquakes in the system that can produce aftershocks. We have chosen to set  $M_{\min}$  to 0, as justified earlier; but since  $M = 0$  is near the lower limit of our observational abilities for tectonic earthquakes, it is rare to observe an aftershock of an  $M = 0$  earthquake. Likewise, it is difficult to observe smaller earthquakes and whether or not they are having aftershocks. Hence the true  $M_{\min}$  could be as high as one or lower than zero. The number of aftershocks that our model predicts are secondary decreases if  $M_{\min}$  is in fact one rather than zero, but the effect is small and is within our current error bars. If  $M_{\min}$  is smaller than zero, the percentage of secondary aftershocks increases, so our result becomes a lower bound on the true percentage.

[42] Our result is also sensitive to our choice of  $b$  value. We used 1.0 for our calculations, but we find that the 65% confidence range of  $b$  values for the Landers sequence is from 0.975 to 1.065. A  $b$  value of 0.975 would correspond to about 5% more of the 7-year Landers aftershocks being secondary; a  $b$  value of 1.065 would correspond to about 15% less secondary activity.

#### 4.1.2. Uniform Aftershock Productivity

[43] Another issue is that our model uses the same equation and basic parameters to build the direct aftershock

sequence of the main shock and the direct aftershock sequences of the aftershocks themselves. For this type of modeling to give us the correct percentage of secondary aftershocks, it is not required that every secondary aftershock sequence exactly mimic the shape of the Landers sequence; there may be large variations between individual sequences, as is regularly observed between aftershock sequences in general. What is required, however, is that there be no systematic tendency for aftershocks to produce their own aftershocks at any faster or slower rate than the main shock that triggered them, after correction for relative magnitudes (see section 2.2).

[44] Is this assumption reasonable? We note that no physical differences have been found between aftershocks and other earthquakes; therefore the total number of faults that an earthquake of a given magnitude can significantly stress is not affected by whether or not it is an aftershock. There may be a difference in the receptivity of those faults, however, given that a large earthquake has just occurred. Indeed, we note that the core region of the Joshua Tree aftershock sequence, although located just south of the Landers fault, showed essentially no change in seismicity rate in response to the Landers earthquake. This suggests either fault exhaustion or some poorly understood indifference to stressing from the Landers earthquake as a result of high stressing from the Joshua Tree earthquake two months earlier. We hypothesize, therefore, that a fault population's prestressing is important. Fault prestressing will not cause systematic differences in the aftershock rates of main shocks and aftershocks, however, if large main shock productivity is affected by previous activity in its aftershock zone to a similar degree to which secondary aftershock productivity is affected by the main shock. Indeed, we have found good evidence that the aftershock rates are similar.

[45] We first note that our model, which assumes that the aftershock rates are the same, fits the data well (Figure 6). Second, an abnormal aftershock production rate has not been observed for secondary aftershock sequences occurring on the edges of aftershock sequences, where they can most easily be separated from other activity (*Page* [1968] and our own observations of the Pisgah aftershock sequence). However, the fault populations at the edges of aftershock zones might not be representative. The strongest evidence comes from foreshock statistics. If aftershocks produce their own aftershocks at a significantly different rate than other earthquakes, then it follows from section 2.4 that the incidence of foreshock occurrence within aftershock sequences should be different from the average. Unfortunately, it is impossible to uniformly inspect large early aftershocks for foreshocks. However, we find that for the California-Nevada data set that we used in section 2, aftershock activity quiets down enough after one month that foreshocks may be identified if we use the conservative criteria that foreshocks must occur within 2 km of a large aftershock and that the foreshock sequences must continue to within 24 hours of the large aftershock. In comparison, the *Abercrombie and Mori* [1994] criterion for foreshock identification (outside of aftershock sequences) is a maximum of 5 km and 30 days of event separation.

[46] Our data set contains 14  $M \geq 5$  earthquakes that occurred as aftershocks of other  $M \geq 5$  earthquakes in a time period spanning from 1 month to 2 years after the

respective main shock. Five of the  $M \geq 5$  earthquakes occurred as aftershocks of  $M$  5–6 main shocks, five as aftershocks of  $M$  6–7 main shocks, and four as aftershocks of  $M \geq 7$  main shocks. Of the aftershocks that we determine to have foreshocks, the average time delay between the foreshocks and the  $M \geq 5$  aftershocks was 3.7 hours. In comparison, the average time delay between the foreshocks and the previous  $M \geq 2$  earthquake within a 9 km radius was 15.6 days. This contrast provides confidence that our foreshock identification criteria are reasonable.

[47] Using the California-Nevada foreshock statistics that we solved for in section 2.4, we predict that if aftershocks trigger their own aftershocks at the same rate as other earthquakes do we should observe that  $2.1 \pm 2.7$  (95% confidence) of the  $M \geq 5$  aftershocks have foreshocks in the range  $M$  4–5; we find two that do. Likewise,  $1.8 \pm 2.5$   $M \geq 5$  aftershocks should have  $M$  3–4 foreshocks; two are observed. Finally,  $1.5 \pm 2.3$   $M \geq 5$  aftershocks should have  $M$  2–3 foreshocks, and again, two are observed. This agreement suggests that aftershocks do not produce their own aftershocks at any significantly different rate than other earthquakes do.

#### 4.2. Implications for Static Stress Triggering Studies

[48] Our analysis suggests that at the time of the Hector Mine earthquake, 82% of ongoing Landers earthquake aftershocks were secondary. We infer that these aftershocks occurred in response to a stress field that had been changed significantly since the time of the Landers main shock. Since the Landers aftershock sequence is not a highly unusual one for southern California, this implies that however well we refine our ability to calculate stress changes caused by large main shocks, and however well we refine our ability to calculate the hypocentral and fault plane parameters of aftershocks, a significant number of aftershocks will remain unpredictable because of our present inability to calculate the stress contributions of the multitude of small aftershocks. These contributions will consist of stress fluctuations at all spatial scales, with each aftershock producing stress changes comparable to those of the main shock but over a spatial domain scaled by its own rupture size.

[49] Calculating main shock-induced stress changes are still useful; many studies have found that such calculations improve our ability to predict where aftershocks occur [e.g., Harris and Simpson, 1992; King et al., 1994; Stein et al., 1997]. We argue that such calculations should, however, be regarded as a first step in predicting earthquake triggering, and that critical next steps are yet to be developed to account for the fact that stress changes produced by aftershocks are significant. Since stress changes from aftershocks accumulate with time, our results imply in particular that short-term stress change results have uncertain relevance for long-term predictions. Indeed, since most aftershocks occur soon after the main shock the results of most stress change studies are dominated by early aftershock statistics. Our model indicates that the percentage of ongoing aftershocks that are secondary climbs quickly during the first several days of a sequence, however, before it levels out asymptotically (Figure 7). (This transition to asymptotic growth occurs because the direct aftershocks decay according to Omori's law, which mandates very slow decay at long time periods. Thus the remaining fraction of

direct aftershocks will force the percentage of secondary aftershocks to level out below 100%.) As a result, we predict that late aftershock populations should show less correlation with main shock stress changes than aftershock populations as a whole. This may explain the findings of Harris et al. [1995] that static Coulomb stress changes caused by  $M \geq 5$  main shocks in California could be used to predict the locations of  $M \geq 5$  earthquakes in California only if less than 1.5 years had elapsed since the last triggering main shock.

[50] We also note that statistical analysis of static stress change predictions have always reflected significant limitations of the technique. This failure is presumably due to some combination of secondary triggering, non-static stress triggering mechanisms (which must effect secondary as well as primary aftershocks) and inaccurate stress change modeling resulting from main shock slip uncertainties, structural inhomogeneities [Langenheim and Jachens, 2000; Hearn, 2001], focal mechanism uncertainties [Kilb, 2001], and other problems. For example, Hardebeck [2001] estimated that for the first month of the Landers aftershock sequence,  $63 \pm 2\%$  of the aftershocks were consistent with the combined static Coulomb stress change induced by the main shock and the largest aftershock (the Big Bear earthquake);  $45 \pm 2\%$  of synthetic randomly generated aftershocks were also consistent with these stress changes. We use  $X$  to represent the percentage of aftershocks explainable by the main shock and Big Bear stress changes calculated and assume that the rest of the aftershocks correlate with the calculated stresses at the random earthquake rate. This gives us  $0.45(1 - X) + X = 0.63$ ;  $X = 0.33$ . When we look at all Landers aftershocks, however, we are including many aftershocks that occurred close to the main shock fault plane, where agreement between aftershocks and main shock stress triggering is often poor, presumably because of uncertainties in the main shock slip inversion. Limiting the data set to aftershocks experiencing between 0.1 and 5 bars of stress change, where Hardebeck [2001] finds the best agreement, we find that 71% of the observed aftershocks and 47% of the randomized catalog agreed with the main shock stress change. This yields  $X = 45\%$ , meaning that 55% of the aftershocks were potentially unrelated to the static stress changes caused by the main shock. In comparison, our simulations predict that 51% of Landers aftershocks occurring in the first month were secondary with respect to the Landers main shock and about 43% of the aftershocks were secondary with respect to both the Landers earthquake and its largest aftershock.

[51] Studies of some other earthquakes reveal even less agreement between aftershocks and main shock-induced static stresses. The results of Hardebeck [2001] for the 1994  $M_W$  6.7 Northridge earthquake, for example, indicate that  $X = 12\%$  for all of the aftershocks and  $X = 26\%$  for the subset experiencing 0.1 to 5 bars of main shock stress change. Toda et al. [1998] compared seismicity rate changes after the 1995 Kobe earthquake with the static stress changes produced by the main shock. For areas experiencing less than 8 bars of stress change, they found that 61% of the seismicity rate changes were consistent with the static stress changes, while 60% were consistent with a null hypothesis motivated by a simple model of dynamic triggering.

[52] These results suggest that we might best predict aftershock locations if we focus both on predictions from stress change studies and on areas where aftershocks are already clustering, which is where secondary aftershocks are most likely to occur. In addition to the Hector Mine earthquake the Landers earthquake itself [Hauksson *et al.*, 1993], the 1999  $M_W$  7.2 Düzce, Turkey [Parsons *et al.*, 2000], and the 1988  $M_W$  7.8 Gulf of Alaska earthquake, among others, nucleated within aftershock clusters of a previous main shock. Spatial variations in aftershock activity may also be used to identify which aftershock clusters are most likely to produce large aftershocks [Wiemer, 2000].

[53] In summary, stress changes from the main shock should dominate the first-order aftershock pattern and hence do have predictive power. However, the aftershocks themselves modify the pattern so significantly that it becomes difficult to test whether specific events are compatible with local stress changes. In particular, we note that this result means that whether or not different aftershock triggering models, such as static Coulomb or viscoelastic stress change, agree with the Hector Mine earthquake, a single triggered event, cannot be used to discriminate between the models. Instead, the clear statistical dominance of one model over another must be demonstrated for large data sets of aftershocks.

## 5. Conclusions

[54] Statistical evidence supports the hypothesis that the magnitude of any single aftershock is statistically independent of the magnitude of its main shock. This means that foreshocks are simply small main shocks that trigger large aftershocks. Hence it is probable that the 1999  $M$  7.1 Hector Mine earthquake was not triggered directly by the 1992  $M$  7.3 Landers earthquake but rather by its own foreshocks, which were themselves triggered directly or indirectly by the Landers earthquake. This could explain why static Coulomb stress change analysis has not been able to determine conclusively whether slip on the Landers main shock fault triggered the Hector Mine earthquake, as the foreshocks and other small earthquakes would have changed the static stress regime in the neighborhood of the Hector Mine earthquake hypocenter.

[55] Monte Carlo simulations and conditional probability imply quantitatively that there is at least an 85% chance that a small aftershock of the Landers earthquake, not the Landers earthquake itself, was the most direct trigger of the Hector Mine earthquake. Our simulations take into account the magnitude of the Landers main shock, the activity level of the aftershock sequence, and the fact that the Hector Mine earthquake occurred 7 years into this sequence. Hence there is only a 15% chance that direct stress from the Landers main shock triggered the Hector Mine earthquake. Thus we urge that at least as much priority be placed on modeling the significant statistical stress fluctuations produced by aftershocks themselves as on refining models of main shock-induced stress changes.

[56] **Acknowledgments.** We would like to thank James Sethna for insightful discussions that provided the foundation for this work and Yu Gu for critical technical help. Ruth Harris and an anonymous reviewer provided constructive reviews that led to significant improvements in the manuscript.

We would also like to thank Debi Kilb, Patricia Moreno, Yu Gu, and James Wang for editing and Herman Chernoff, David Vere-Jones, Jun Liu, Alan Kafka, John Ebel, Elizabeth Marrin, and Nadia Lapusta for helpful discussions. We are grateful for earthquake catalog data made available by the Council of the National Seismic System, the Southern California Earthquake Data Center, California Institute of Technology, the Northern California Earthquake Data Center, the Berkeley Seismological Laboratory, and the Northern California Seismic Network. K.R.F. was supported by an NSF graduate student fellowship and T.W.B. was supported by a DAAD Doktorandenstipendium under the HSP-III program. Additional support was provided by National Science Foundation grant EAR-98-05172 and the Southern California Earthquake Center. This is SCEC contribution 613, funded by NSF cooperative agreement EAR-89290136 and USGS cooperative agreements 14-08-0001-A0899 and 1434-HQ-97AG01718.

## References

- Abercrombie, R. E., Earthquake source scaling relationships from  $-1$  to 5  $M_L$  using seismograms recorded at 2.5-km depth, *J. Geophys. Res.*, **100**, 24,015–24,036, 1995.
- Abercrombie, R. E., and J. Mori, Local observations of a large earthquake: 28 June 1992, Landers, California, *Bull. Seismol. Soc. Am.*, **84**, 725–734, 1994.
- Abercrombie, R. E., and J. Mori, Occurrence patterns of foreshocks to large earthquakes in the western United States, *Nature*, **381**, 303–307, 1996.
- Agnew, D. C., and L. M. Jones, Prediction probabilities from foreshocks, *J. Geophys. Res.*, **96**, 11,959–11,971, 1991.
- Båth, M., Lateral inhomogeneities in the upper mantle, *Tectonophysics*, **2**, 483–514, 1965.
- Beroza, G. C., and M. D. Zoback, Mechanism diversity of the Loma Prieta aftershocks and mechanics of mainshock-aftershock interaction, *Science*, **259**, 210–213, 1993.
- Console, R., and M. Murru, A simple and testable model for earthquake clustering, *J. Geophys. Res.*, **106**, 8699–8711, 2001.
- Dodge, D. A., G. C. Beroza, and W. C. Ellsworth, Foreshock sequence of the 1992 Landers, California, earthquake and its implications for earthquake nucleation, *J. Geophys. Res.*, **100**, 9865–9880, 1995.
- Dodge, D. A., G. C. Beroza, and W. L. Ellsworth, Detailed observations of California foreshock sequences: Implications for the earthquake initiation process, *J. Geophys. Res.*, **101**, 22,371–22,392, 1996.
- Drakatos, G., and L. Latoussakis, A catalog of aftershock sequences in Greece (1971–1997): Their spatial and temporal characteristics, *J. Seismol.*, **5**, 137–145, 2001.
- Dziewonski, A. M., G. Ekström, and M. P. Salganik, Centroid-moment tensor solutions for April–June 1992, *Phys. Earth Planet. Inter.*, **77**, 151–163, 1993.
- Eneva, M., and G. L. Pavlis, Application of pair analysis statistics to aftershocks of the 1984 Morgan Hill, California, earthquake, *J. Geophys. Res.*, **93**, 9113–9125, 1988.
- Freed, A. M., and J. Lin, Delayed triggering of the 1999 Hector Mine earthquake by viscoelastic stress transfer, *Nature*, **411**, 180–182, 1999.
- Gutenberg, B., and C. F. Richter, Frequency of earthquakes in California, *Bull. Seismol. Soc. Am.*, **34**, 185–188, 1944.
- Hanks, T. C., Small earthquakes, tectonic forces, *Science*, **256**, 1430–1432, 1992.
- Hanks, T. C., and D. M. Boore, Moment-magnitude relations in theory and practice, *J. Geophys. Res.*, **89**, 6229–6235, 1984.
- Hardebeck, J. L., The crustal stress field in southern California and its implications for fault mechanics, Ph.D. thesis, 148 pp., Calif. Inst. of Technol., Pasadena, 2001.
- Harris, R. A., Did the 1999 Hector Mine earthquake occur in the stress shadow of the 1992 Landers earthquake? (abstract), *Eos Trans. AGU*, **81**(48), Fall Meet. Suppl., Abstract S62C-09, 2000.
- Harris, R. A., Stress triggers, stress shadows, and seismic hazard, in *IASPEI Seismology Handbook*, edited by W. H. K. Lee, H. Kanamori, and P. Jennings, in press, Int. Assoc. of Seismol. and Phys. Of Earth's Inter., Boulder, Colo., 2002.
- Harris, R. A., and S. M. Day, Dynamics of fault interaction: Parallel strike-slip faults, *J. Geophys. Res.*, **98**, 4461–4472, 1993.
- Harris, R. A., and R. W. Simpson, Changes in static stress on southern Californian faults after the 1992 Landers earthquake, *Nature*, **360**, 251–254, 1992.
- Harris, R. A., and R. W. Simpson, The 1999  $M_W$  7.1 Hector Mine, California earthquake—A test of the stress shadow hypothesis?, *Bull. Seismol. Soc. Am.*, **4**, 1497–1512, 2002.
- Harris, R. A., R. W. Simpson, and P. A. Reasenber, Influence of static stress changes on earthquake locations in southern California, *Nature*, **375**, 221–224, 1995.
- Hauksson, E., State of stress from focal mechanisms before and after the 1992 Landers earthquake sequence, *Bull. Seismol. Soc. Am.*, **84**, 917–934, 1994.

- Hauksson, E., L. M. Jones, K. Hutton, and D. Eberhart-Phillips, The 1992 Landers earthquake sequence: Seismological observations, *J. Geophys. Res.*, *98*, 19,835–19,858, 1993.
- Hearn, E. H., Estimating coseismic slip and crustal stress changes from surface displacement data and elastically layered Earth models: Findings from the 1999 Izmit, Turkey earthquake (abstract), *Eos Trans. AGU*, *82*(47), Fall Meet. Suppl., Abstract S11C-01, 2001.
- Hurukawa, N., The 1995 Off-Etorofu earthquake: Joint relocation of foreshocks, the mainshock, and aftershocks and implications for the earthquake nucleation process, *Bull. Seismol. Soc. Am.*, *88*, 1112–1126, 1998.
- Jones, L. M., Foreshocks (1966–1980) in the San Andreas system, California, *Bull. Seismol. Soc. Am.*, *74*, 1361–1380, 1984.
- Jones, L. M., and P. Molnar, Some characteristics of foreshocks and their possible relationship to earthquake prediction and premonitory slip on faults, *J. Geophys. Res.*, *84*, 3596–3608, 1979.
- Kagan, Y. Y., Likelihood analysis of earthquake catalogs, *Geophys. J. Int.*, *106*, 135–148, 1991.
- Kagan, Y. Y., and L. Knopoff, Stochastic synthesis of earthquake catalogs, *J. Geophys. Res.*, *86*, 2853–2862, 1981.
- Kanamori, H., The energy release in great earthquakes, *J. Geophys. Res.*, *82*, 2981–2987, 1977.
- Kanamori, H., and D. L. Anderson, Theoretical basis of some empirical relations in seismology, *Bull. Seismol. Soc. Am.*, *65*, 1073–1095, 1975.
- Kilb, D., The Landers and Hector Mine earthquakes: Correlations between dynamic stress changes and earthquake triggering (abstract), *Eos Trans. AGU*, *81*(48), Fall Meet. Suppl., Abstract S62C-10, 2000.
- Kilb, D., Fault parameter constraints using relocated earthquakes: Implications for stress change calculations, *Eos Trans. AGU*, *82*(47), Fall Meet. Suppl., Abstract S11C-10, 2001.
- Kilb, D., and J. Gomberg, The initial subevent of the 1994 Northridge, California earthquake: Is earthquake size predictable?, *J. Seismol.*, *3*, 409–420, 1999.
- King, G. C. P., R. S. Stein, and J. Lin, Static stress change and the triggering of earthquakes, *Bull. Seismol. Soc. Am.*, *84*, 935–953, 1994.
- Kurimoto, H., A statistical study of some aftershock problems, *J. Seismol. Soc. Jpn.*, *12*, 1–10, 1959.
- Langenheim, V. E., and R. C. Jachens, A link between the Landers and Hector Mine earthquakes, southern California, inferred from gravity and magnetic data, *Eos Trans. AGU*, *81*(48), Fall Meet. Suppl., Abstract S62C-02, 2000.
- Lapusta, N., J. R. Rice, Y. Ben-Zion, and G. Zheng, Elastodynamic analysis for slow tectonic loading with spontaneous rupture episodes on faults with rate- and state-dependent friction, *J. Geophys. Res.*, *105*, 23,765–23,789, 2000.
- Michael, A. J., and L. M. Jones, Seismicity alert probabilities at Parkfield, California, revisited, *Bull. Seismol. Soc. Am.*, *88*, 117–130, 1998.
- Mori, J., Rupture directivity and slip distribution of the  $M$  4.3 foreshock to the 1992 Joshua Tree earthquake, southern California, *Bull. Seismol. Soc. Am.*, *86*, 805–810, 1996.
- Mori, J., and H. Kanamori, Initial rupture of earthquakes in the 1995 Ridgecrest, California, sequence, *Geophys. Res. Lett.*, *23*, 2437–2440, 1996.
- Ogata, Y., Space-time point-process models for earthquake occurrences, *Ann. Stat.*, *50*, 379–402, 1998.
- Page, R., Aftershocks and microaftershocks of the great Alaska earthquake of 1964, *Bull. Seismol. Soc. Am.*, *58*, 1131–1168, 1968.
- Parsons, T., and D. Dreger, Static-stress impact of the 1992 Landers earthquake sequence on nucleation and slip at the site of the 1999  $M = 7.1$  Hector Mine earthquake, southern California, *Geophys. Res. Lett.*, *27*, 1949–1952, 2000.
- Parsons, T., S. Toda, R. S. Stein, A. Barka, and J. H. Dieterich, Heightened odds of large earthquakes near Istanbul; an interaction-based probability calculation, *Science*, *288*, 661–665, 2000.
- Pollitz, F. F., and I. S. Sacks, Stress triggering of the 1999 Hector Mine earthquake by transient deformation following the 1992 Landers earthquake, *Bull. Seismol. Soc. Am.*, *4*, 1487–1496, 2002.
- Price, E. J., and R. Bürgmann, Interactions between the Landers and Hector Mine, California, earthquakes from space geodesy, boundary element modeling, and time-dependent friction, *Bull. Seismol. Soc. Am.*, *4*, 1450–1469, 2002.
- Reasenber, P. A., Foreshock occurrence before large earthquakes, *J. Geophys. Res.*, *104*, 4755–4768, 1999.
- Reasenber, P. A., and L. M. Jones, Earthquake hazard after a mainshock in California, *Science*, *243*, 1173–1176, 1989.
- Richardson, E., and T. H. Jordan, Seismicity in deep gold mines of South Africa: Implications for tectonic earthquakes, *Bull. Seismol. Soc. Am.*, in press, 2002.
- Richter, C. F., *Elementary Seismology*, 768 pp., W. H. Freeman, New York, 1958.
- Robertson, M. C., C. G. Sammis, M. Sahimi, and A. J. Martin, Fractal analysis of three-dimensional spatial distributions of earthquakes with a percolation interpretation, *J. Geophys. Res.*, *100*, 609–620, 1995.
- Rubinstein, R. Y., *Simulation and the Monte Carlo Method*, 278 pp., John Wiley, New York, 1981.
- Sauber, J., W. Thatcher, S. C. Solomon, and M. Lisowski, Geodetic slip rate for the eastern California shear zone and the recurrence time of Mojave Desert earthquakes, *Nature*, *367*, 264–266, 1994.
- Stein, R. S., A. Barka, and J. Dieterich, Progressive failure on the North Anatolian fault since 1939 by earthquake stress triggering, *Geophys. J. Int.*, *128*, 594–604, 1997.
- Toda, S., R. S. Stein, P. A. Reasenber, J. H. Dieterich, and A. Yoshida, Stress transferred by the 995  $M_W = 6.9$  Kobe, Japan, shock: Effect on aftershocks and future earthquake probabilities, *J. Geophys. Res.*, *103*, 24,543–24,565, 1998.
- Tsapanos, T. M., Spatial distribution of the difference between the magnitudes of the mainshock and the largest aftershock in the circum-Pacific belt, *Bull. Seismol. Soc. Am.*, *80*, 1180–1189, 1990.
- Utsu, T., A statistical study on the occurrence of aftershocks, *Geophys. Mag.*, *30*, 521–605, 1961.
- Vere-Jones, D., A note on the statistical interpretation of Båth's law, *Bull. Seismol. Soc. Am.*, *59*, 1535–1541, 1969.
- Wiemer, S., Introducing probabilistic aftershock hazard mapping, *Geophys. Res. Lett.*, *27*, 3405–3408, 2000.
- Yamanaka, Y., and K. Shimazaki, Scaling relationship between the number of aftershocks and the size of the mainshock, *J. Phys. Earth*, *38*, 305–324, 1990.
- Zeng, Y., Viscoelastic stress-triggering of the 1999 Hector Mine earthquake by the 1992 Landers earthquake, *Geophys. Res. Lett.*, *28*, 3007–3010, 2001.

---

R. E. Abercrombie, T. W. Becker, G. Ekström, and K. R. Felzer, Department of Earth and Planetary Sciences, Harvard University, Cambridge, MA 02138, USA. (felzer@seismology.harvard.edu)  
 J. R. Rice, Division of Engineering and Applied Sciences, Harvard University, Cambridge, MA 02138, USA.